ELSEVIER J. Non-Newtonian Fluid Mech., 60 (1995) 259–275

Journal of Non-Newtonian Fluid Mechanics

A thixotropy model for coal–water mixtures

Hiromoto Usui

Department of Applied Chemistry and Chemical Engineering, Yamaguchi University, Tokiwadai, Ube 755, Japan

Received 18 April 1995; in revised form 14 July 1995

Abstract

The thixotropy model developed in this study is based on the phenomenological scheme proposed by Cheng and Evans, Brit. J. Appl. Phys., 16 (1965) 1599–1617. The idea of this model is based on the assumption that the thixotropic behavior of dispersed systems is well described by the coagulation process of the minimum sized particles contained in a dispersion system and the break-up process of coagulated clusters. Combined with the modified-cell model, the proposed thixotropy model can predict the complex rheological behavior of coal–water mixtures. This model can be applied to predict the viscosity of highly concentrated solid–liquid dispersion systems which have a wide particle-size distribution.

Keywords: Alternative fuel; Coal; Slurry; Suspension; Thixotropy

1. Introduction

Coal water mixtures (CWMs) [1–4] have been given considerable attention as an alternative fuel. However, the rheological behavior of CWMs is complicated. Development of a precise method of predicting CWM rheology has been one of the main subjects in the field of CWM technology. Usui and Sano [5] have proposed a phenomenological thixotropy model in which an internal structural stress was taken as a thixotropic parameter. This model was based on the phenomenological scheme proposed by Cheng and Evans [6]. Although this model was successfully employed to evaluate the sedimentation stability of CWMs [7], the physical meaning of the internal structural stress was not clear. Thus, the present investigation is aimed at proposing a more sophisticated thixotropy model which has a better physical

SSDI 0377-0257(95)01383-0

understanding. The present model has been developed to satisfy the following requirements.

(1) The model can be applied to a slurry which has a particle-size distribution.
(2) The model is applicable to highly concentrated slurries.
(3) The change of surface characteristics caused by the additives can be taken into account.
(4) Time-dependent rheological characteristics (i.e. thixotropy) of slurries can be expressed by the model.

However, the effect of the non-spherical nature of the particles and the friction caused by the particle collisions are not taken into account in the present model.

2. Thixotropy model

In the following discussion, the basis of calculation will be 1 m^3 of CWM. The solid volume fraction, ϕ, solid weight concentration, c_w, solid density, ρ_s, are already specified. Also, the number-based particle size distribution, N_0, $N_1 \cdots N_{max}$, is specified for each particle size, $d_0, d_1 \cdots d_{max}$, where d_0 and d_{max} are minimum and maximum particle size, respectively. A typical particle size distribution is shown in Table 1. It is evident that the number of the minimum-sized particles, N_0, is much larger than $N_1, N_2 \cdots N_{max}$. Thus we assume that only the minimum size particles can coagulate to produce clusters. Particles larger than the minimum-sized particle do not interact with each other.

We also assume that the coagulated minimum size particles produce a spherical cluster, and that the behavior of this cluster is the same as that of a solid particle with the same diameter. Now, let us choose the number of minimum particles contained in a cluster, n, as a thixotropy parameter. The coagulation process in a cluster may be described by a Brownian coagulation and shear coagulation process.

Table 1
Particle size distribution of a CWM (CWM-A2)

d (μm)	X_i (−)	N_i
0.56	0.0529	3.56×10^{17}
1.79	0.0484	9.97×10^{15}
3.19	0.0634	2.31×10^{15}
5.70	0.0972	6.20×10^{14}
10.2	0.139	1.54×10^{14}
18.2	0.177	3.46×10^{13}
32.4	0.188	6.53×10^{12}
57.9	0.143	8.74×10^{11}
100	0.0644	7.60×10^{10}
150	0.0245	8.58×10^{9}
300	0.0022	8.58×10^{9}

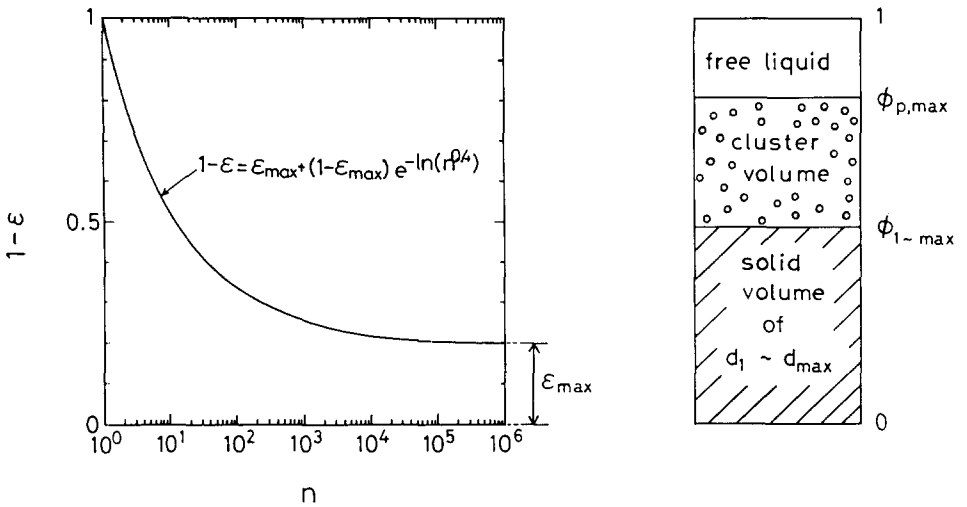

Fig. 1. Void fraction in a cluster as a function of the number of minimum-sized particles contained in a cluster.

We adopt the formulation proposed by previous papers [8,9], and after some algebraic manipulation, we obtain

$$\frac{dn}{dt} = \frac{4\alpha_b k_B T N_0}{3\eta_0} + \frac{4\alpha_s \phi \dot{\gamma} n}{\pi}, \tag{1}$$

where t is time, α_b is a constant ($\alpha_b = 0.58$) for Brownian coagulation, k_B is the Boltzmann constant, T is temperature, α_s is a constant ($\alpha_s = 0.6$) for shear coagulation, ϕ is the solid volume fraction, $\dot{\gamma}$ is the shear rate, and η_0 is the solvent viscosity, respectively.

The break-up process model is proposed in this study. As the number of minimum size particles was previously defined as N_0, the number of clusters is given by

$$N_c = N_0/n. \tag{2}$$

The void ratio, ϵ, is defined as the ratio of solvent volume to the solid volume in a cluster. Thus, the volume of a cluster, v_c, is given by

$$v_c = \frac{n}{1-\epsilon}\frac{\pi}{6} d_0^3, \tag{3}$$

and the total volume of clusters, V_c, is given by

$$V_c = v_c N_c. \tag{4}$$

When the minimum-sized particles are completely dispersed, i.e. at $n = 1$, ϵ must be equal to zero. For a given particle size distribution, the maximum packing volume fraction, $\phi_{p,max}$, is calculated by a suitable method. Here the algorithm proposed by Lee [10] will be used to predict the value of $\phi_{p,max}$. Let the solid volume fraction of particles with diameters d_1–d_{max} be ϕ_{1-max}. We assume that the volume fraction,

$\phi_{p,\max} - \phi_{1-\max}$ is occupied by one cluster at the limiting condition that $n \to \infty$ as shown in Fig. 1. Thus the cluster void fraction, $\epsilon_{\max}$, at $n \to \infty$ is given by

$$1 - \epsilon_{\max} = 1 - \frac{N_0(\pi/6)d_0^3}{\phi_{p,\max} - \phi_{1-\max}}. \tag{5}$$

This packing condition corresponds to very loose packing. Although we can obtain the limiting values of ϵ both at $n = 1$ and $n = \infty$, the dependence of ϵ on the number of minimum size particles contained in a cluster is not completely understood. Thus we assume the following dependence of the void fraction, ϵ, on n:

$$1 - \epsilon = \epsilon_{\max} + (1 - \epsilon_{\max}) \exp(-\ln n^{0.4}). \tag{6}$$

The profile of $(1 - \epsilon)$ is shown in Fig. 1. There is no information on the functional dependence of ϵ on n in the intermediate stage. More discussion on the assumed profile will be provided in a future study.

The cluster subject to simple shear flow may be deformed by the shear, and finally it may be subdivided into smaller clusters. The deformation and break-up process of clusters in the simple shear flow was discussed by Smith and van de Ven [11]. However, it is very difficult to decide which break-up process corresponds to the case of clusters in a CWM. Thus, we adopt the simple assumption that the cluster deforms and finally breaks up into two equally sized fragments when subjected to shear. Also, it is assumed that there is no resistance during the cluster deformation process shown in Fig. 2. Next, a more simplified cluster break-up process is assumed as shown in Fig. 3. The clusters just before break-up are connected only by a single bond. The shear flow fleld is approximated by a step change of the velocity profile rather than the simple shear flow as shown in Fig. 3. Let the cluster diameter before the break-up be equal to d_c. As the cluster is subdivided into two clusters of the same diameter, d'_c, we have the following relationship between these two diameters:

$$d'_c = d_c/2^{1/3}. \tag{7}$$

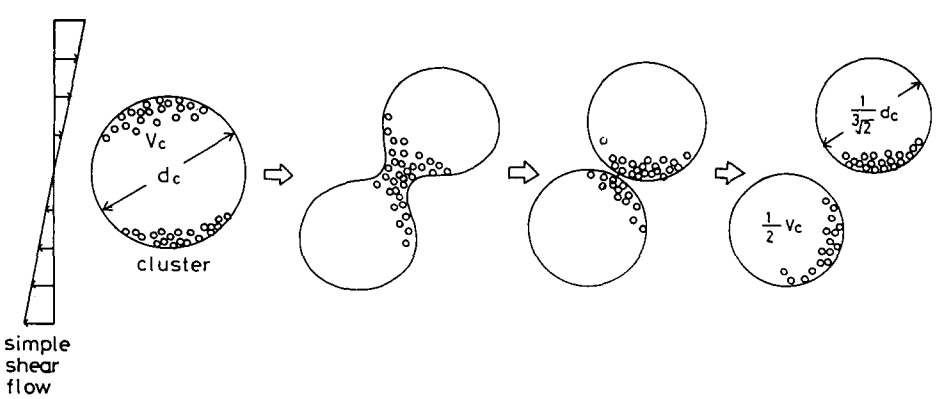

Fig. 2. Break-up of a cluster under simple shear flow.

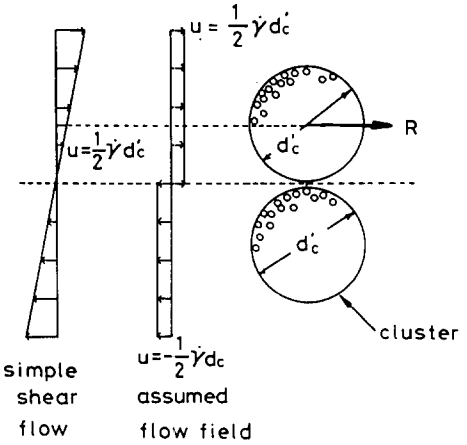

Fig. 3. Idealized shear break-up of a cluster.

The drag force, R, acting on the cluster is expressed as

$$R = C_R(\pi/4)d_c'^2\rho_f u^2/2, \tag{8}$$

where u is assumed to be equal to $\dot{\gamma}d_c'/2$. Assuming that Stokes' law is applicable (i.e. $C_R = 24/Re$, $Re = \rho_f d_c' u/\eta$) to each cluster, the moment, M, acting at the bonding point is given by

$$M = 2\frac{d_c'}{2}R$$

$$= \frac{9}{2}v_c\eta\dot{\gamma}, \tag{9}$$

where v_c is the volume of a cluster before the break-up. The above discussion cannot be applied in the case of a single solid particle (i.e. at $n = 1$), because it is impossible to break up a single solid particle. v_c should be defined as the cluster volume to be subdivided. In other words, v_c must be zero if $n = 1$. So, we define, hereafter, the cluster volume as

$$v_c = \frac{n}{1-\epsilon}\frac{\pi}{6}d_0^3 - \frac{\pi}{6}d_0^3 = \frac{\pi}{6}d_0^3\left(\frac{n}{1-\epsilon} - 1\right). \tag{10}$$

Now, let us define the inter-particle bonding energy as F_0, and the total bonding number per unit volume of slurry as X. X is expressed by

$$X = N_0 - N_t = N_0(n-1)/n, \tag{11}$$

where the number of clusters is defined by $N_t = N_0/n$. The term, $-F_0\,dX/dt$ $(= -F_0(N_0/n^2)\,dn/dt)$, is the total energy needed to break-up the cluster bonding per unit volume and per unit time. The volumetric flow rate which passes the unit volume of slurry is given by $\dot{\gamma}/2$. Then, the cluster number included in the incoming flow is equal to $\dot{\gamma}N_t/2$. Taking account of the moment exerted on the cluster given

by Eq. (9), the energy balance between the total drag force and the total bond break-up energy results in

$$-F_0 \frac{N_0}{n^2}\frac{dn}{dt} = 2\frac{d'_c}{2} R \frac{1}{2}\dot{\gamma} N_t. \tag{12}$$

Combining the above expression for the break-up process with the Brownian and shear coagulation equation given by Eq. (1), the final rate equation of n can be expressed as

$$\frac{dn}{dt} = \frac{4\alpha_b k_B T N_0}{3\eta_0} + \frac{4\alpha_s \phi \dot{\gamma} n}{\pi} - \frac{3\pi d_0^3 n}{8F_0}\left(\frac{n}{1-\epsilon} - 1\right)\eta\dot{\gamma}^2, \tag{13}$$

where η is taken as the CWM viscosity at $n = 1$. The predicted results using Eq. (13) will be discussed in the Section 3.

3. Modified cell model

It is necessary to develop a method that calculates the viscosity of a CWM using the value of n predicted by Eq. (13). For this purpose, the present authors attempted to modify the cell model proposed by Happel [12]. The cell model given by Happel is summarized as follows:

$$\eta = \eta_0(1 + 5.5\gamma^3\psi), \tag{14}$$

where

$$\psi = \frac{4\gamma^7 + 10 - (84/11)\gamma^2}{10(1-\gamma^{10}) - 25\gamma^3(1-\gamma^4)}, \tag{15}$$

and γ $(=a/b)$ is the ratio of particle radius, a, to the cell radius, b. The cell model has been successfully applied to predict the suspension viscosity of uniform particles. We assume that the value of γ is constant for all particles including a cluster as shown in Fig. 4. At a sufficiently high shear rate region, the rheogram of a suspension generally shows Newtonian viscosity. This means that the cluster is completely broken, and $n = 1$ under this condition. If it is assumed that the flow inside a cell is not affected by the outer flow, including neighbouring particles when

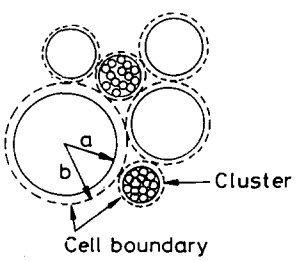

Fig. 4. Particle and cluster images with the cell.

the total cell volume is equal to the maximum packing volume fraction, $\phi_{p,max}$, the value of γ is determined by

$$\gamma = \left(\frac{\phi_{p,max}}{\sum_{i=0}^{max} \pi/6 d_i^3 N_i} \right)^{1/3} . \tag{16}$$

The maximum packing volume fraction, $\phi_{p,max}$ is calculated by Lee's algorithm [10]. Then, the suspension viscosity is predicted by using Eqs. (14–16). The above mentioned procedure can take into account the effect of solid concentration and particle size distribution. However, the effects of inter-particle collision and of surface characteristics are not included. The cell thickness may change slightly depending on surface conditions. Thus, it is assumed that the value of γ is changed by the factor α. We will use $\alpha\gamma$ in Eq. (15) instead of γ. If one set of viscosity and shear rate data for a CWM is experimentally given at sufficiently high sher rates, the value of α can be determined from Eqs. (14–16) assuming that $n = 1$.

In Section 2 it was assumed that the minimum-sized particles coagulated to make clusters. The existence of clusters causes a change in the particle size distribution. So, we should use the term in Eq. (16), $\Sigma_{i=1}^{max} \pi/6 d_i^3 N_i + \pi/6 d_c^3 N_c$, instead of the term; $\Sigma_{i=0}^{max} \pi/6 d_i^3 N_i$, where d_c and N_c are the cluster diameter and the cluster number. The cluster number is easily calculated by N_0/n. The cluster diameter is calculated by means of the void fraction expression given by Eq. (6). In conclusion, the viscosity of a CWM can be estimated if the number of minimum size particle in the cluster is known by the thixotropy model given by Eq. (13).

4. Experiments

4.1. CWM preparation

The CWMs used in this study were prepared as follows. Sample coal was pulverized by two-stage wet mills. Fine and coarse coal samples were mixed to give an optimum particle size distribution [13]. The pulverized coal was mixed with water and additives. Details of the CWMs prepared in this study are summarized in Table 2. The particle size distribution of pulverzied coal was measured by means of a Microtrack Particle Size Analyzer, Model 7995-10. The measured particle size distribution was fitted to the Rossin–Rammler particle size equation, $D = 100$ $[1 - \exp(-bd_p^n)]$, where $D(\%)$ is cumulative under size and $d_p(\mu m)$ is the particle size. The particle size distribution of Buller coal was expressed by the Rossin–Rammler equation as $D = 100$ $[1 - \exp(-0.047 d_p^{0.9})]$. The second sample was prepared by mixing two coal types, Hunter Valley coal and Prima coal (mixing ratio = 4:1). A coarse particle sample of this mixed coal had a particle size distribution given by $D = 100[1 - \exp(-0.030 d_p^{0.9})]$, while the particle size distribution of the fine particle sample was expressed by $D = 100$ $[1 - \exp(-0.08 d_p^{1.2})]$. These coarse and fine particle samples were mixed at a ratio 80.5:19.5 to obtain the optimum particle size distribution.

Table 2
CMWs used in this study

	Coal	Dispersion additive (wt.%/slurry)	Stabilizing additive (wt.%/slurry)	Coal concentration (wt.%)
CWM-A1 [a]	Buller	NSF [e] (0.03)	Guar gum (0.013)	68.2
CWM-A2 [b]				
CWM-A3 [c]				
CWM-A4			Xhantan gum (0.013)	59.7–66.0
CWM-B1 [d]	Hunter Valley	PMA [f] (0.03)	Rhamsan gum (0.03)	58.0
CWM-B2 [d]	+ Prima			58.0
CWM-B3 [d]	(4:1)			58.0

[a] pH 8.1. [b] pH 9.4. [c] pH 10.1.
[d] Details of particle size distributions are given in Section 4.2.
[e] NSF, a condensation product of formalin and naphthalene sulfonic acid.
[f] PMA, polymethacrylate.

4.2. Rheological measurements

The principal experimental tool used in this study is a rheometer (Iwamoto Seisakusho Co., Ltd. model IR-200) with coaxial rotating cylinders. Because the CWM contains solid particles, the clearance between cup and bob has to be maintained sufficiently wide. The maximum particle size of CWMs was 300–500 μm, and the clearance was 6 mm. Although the clearance is not so large compared with the maximum particle size, the ratio of the clearance to the 50% passed diameter of CWMs was around 300. The revolution speed can be changed with a constant revolution gradient in addition to an instant increase and or decrease of revolution speed. The temperature of the test CWM was maintained at 298 K with an air bath.

5. Results and discussion

5.1. Effect of selection in discrete particle size distribution

As a first step for the thixotropy calculation proposed in this study, the particle size distribution must be divided into discrete sizes. If there is a significant effect of division on the predicted results, it is difficult to obtain a general conclusion from the model of this study. Thus it is important to discuss the effect of the division. For this purpose, CWM-A2 was used as a CWM sample. The particle size distribution of CWM-A2 was divided in various ways as shown in Fig. 5. PSD-1 is a standard division. PAD-2 and PSD-3 are used to discuss the effect of the selection of minimum-sized particle effect on the prediction of CWM rheology. The mini-

mum size of the particles is increased for PSD-4 by including the fraction of 1 μm particle. On the other hand, PSD-5 means that the fraction of intermediate particle size is changed. The final example, PSD-6, shows a roughly divided particle size distribution.

The experimental results of the flow curve are shown in Fig. 6. The open circles represent an equilibrium stress level obtained for CWM-A2. A constant shear rate was maintained until an equilibrium condition was achieved. We choose the viscosity data of CWM-A2 at shear rate = 124 s^{-1}. Assuming that $n = 1$, the modified cell model proposed in this study determines the value of α as 1.027. We adopt one more data set of the same solid concentration in the lower shear rate region. For example, adopting the following data set; $\tau = 2.44$ Pa at $\dot{\gamma} = 3.11$ s^{-1}, the number of minimum particles in a cluster is calculated as $n = 14.7$. The modified cell model and Eq. (6) was used for this calculation with the value of $\alpha = 1.027$. Under this shear rate condition, the rate of coagulation must be balanced to the rate-of-shear break-up term. Thus putting $dn/dt = 0$ in Eq. (13), the inter-particle bonding energy F_0 was determined as 2.16×10^{-18} J. Once we obtain the value of F_0 and α, the value of n for different shear rates can be calculated by Eq. (13). The number of minimum-sized particles contained in a cluster increases according to the decrease in shear rate. It is expected that the number, n, becomes infinitely large in the very small shear rate region. Next, the apparent viscosity for each shear rate is calculated by the modified cell model mentioned above. The calculation procedure mentioned here will commonly be employed in the following discussion. Thus, the

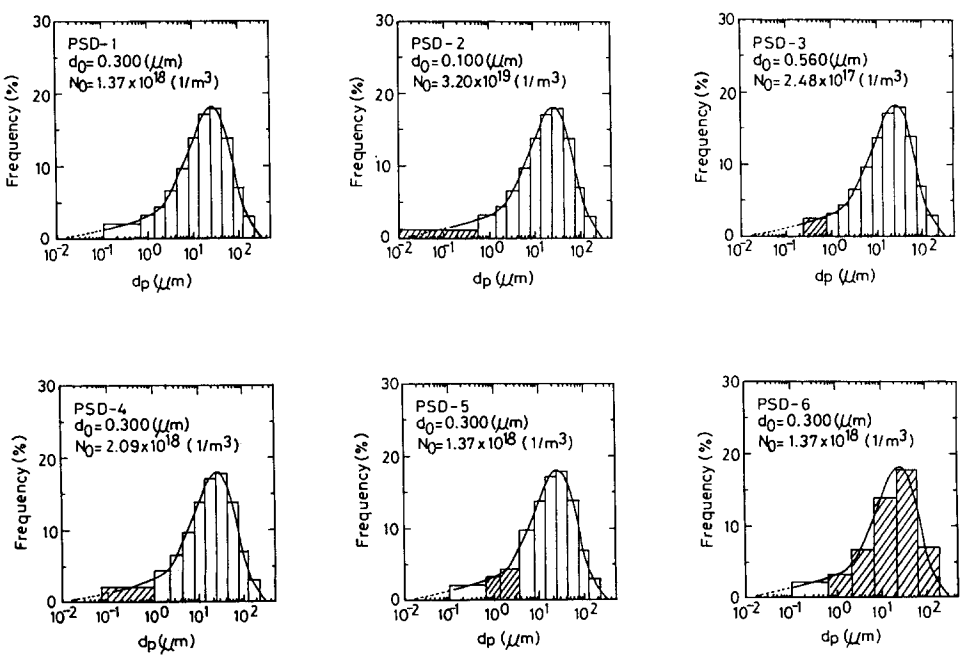

Fig. 5. Examples of discrete particle size distributions for the test of division method.

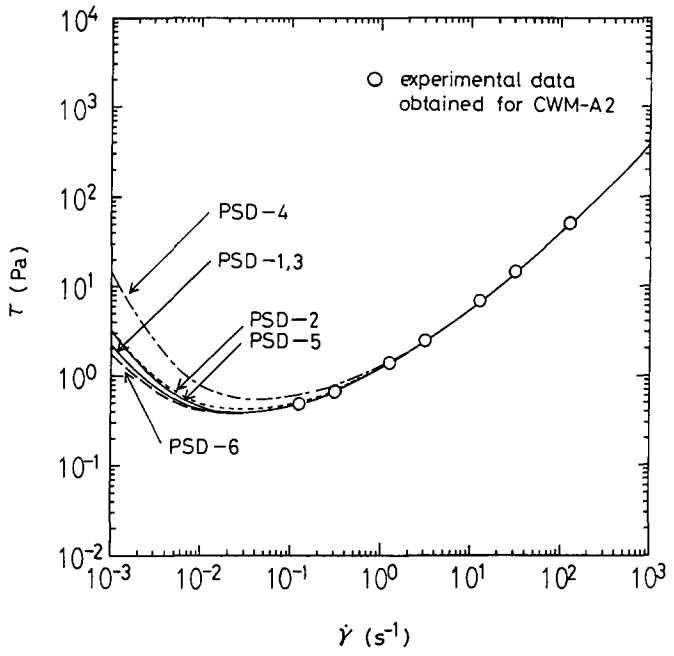

Fig. 6. Effect of division of particle size distribution on the prediction of a flow curve for CWM-A2.

detailed calculation procedure will not be repeated hereafter. The final results of model parameters determined by the present model and the predicted results only will be shown.

Calculated results of the equilibrium stress level for CWM-A2 are compared with measurements in Fig. 6. Agreement between the predictions and experimental data is good for the higher shear rate regions, except the case of PSD-4. Thus we can conclude that the division of particle size distribution is rather insensitive for the prediction of the flow curve at shear rate range larger than 0.1 s^{-1}. If the minimum size particles are artificially increased by including the fraction of other particle sizes (e.g. PSD-4), an anomalous increase in shear stress level at lower shear rate regions is observed. This anomalous behavior of shear stress increase is observed more or less for all particle size distributions. Cluster size becomes infinitely large in the present model, which corresponds to the infinite stress level at the very low shear rate region. Probably, the constant value of F_0 may not be applicable for such a low shear rate range. Also, the spherical cluster assumed in this study no longer exists. Thus we have to conclude that the present model is effective at the shear rate region of $\dot{\gamma} > 0.1$ s^{-1}. So far as we discuss the flow behavior of CWM in such a shear rate region, the division method of particle size distribution to give discrete portions is insensitive to the final prediction, if we do not artificially increase the number of submicron particles.

5.2. Effect of particle size distribution

Three samples of CWM (CWM-B1, B2 and B3) with different particle size distributions were prepared. The CWM-B1 is a coarse particle sample, while CWM-B2 is a mixture of coarse and fine particle samples. The mixing ratio of coarse and fine particle samples was 8:2. 60% of the coarse particle sample was mixed with 40% of fine the particle particle sample in the case of CWM-B3. Particle size distributions of these three samples are shown in Fig. 7. The corresponding flow curves of these CWMs were measured as shown in Fig. 8. The value of α, as expected, is difficult for different CWMs. Thus, α was determined for each CWM by means of the modified cell model, following the procedure mentioned in the previous section. Results are shown in Table 3. Also, F_0 was determined for CWM-B2 as 6.01×10^{-18} J. It was assumed F_0 remained constant because the surface condition was the same for these three CWMs. Predicted results are compared in Fig. 8 showing a good agreement with experimental results. It may be concluded that once we obtain the value of F_0 for a CWM, we can estimate the effect of particle size distribution on CWM rheology. Because the change of α is very small as shown in Table 3, we may use a constant value of α.

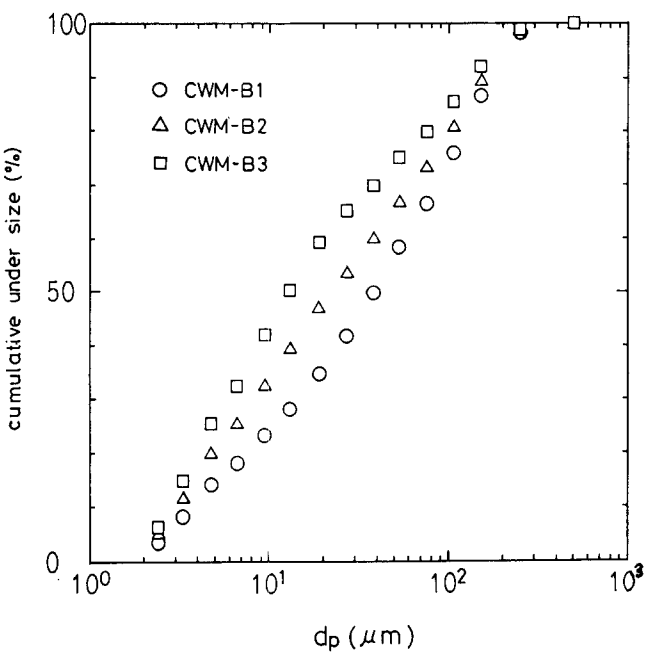

Fig. 7. Particle size distributions of CWM-B1, B2 and B3.

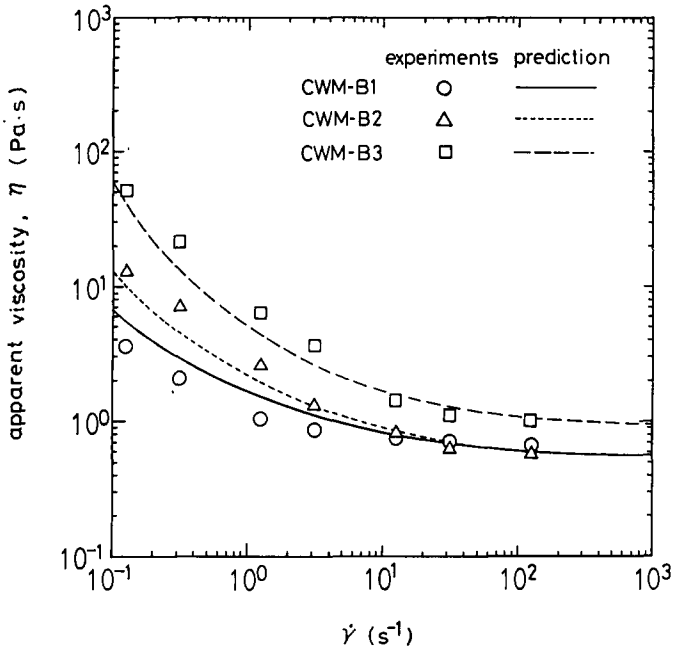

Fig. 8. Prediction of apparent viscosity of CWM-B1, B2 and B3, and its comparison with the experimental results.

5.3. *Effect of coal concentration on CWM viscosity*

The coal concentration of CWM-A4, C_w, was varied from 59.7% to 66.0%. Shear stress vs. shear rate relationships measured by a rheometer and a capillary viscometer are shown in Fig. 9. Using the viscosity data of 65 wt.% CWM at higher shear rate region, the value of α was determined by the modified cell model as $\alpha = 1.052$. Also, the value of F_0 was determined from the viscosity data in the intermediate shear rate region as $F_0 = 1.00 \times 10^{-17}$ J. These values are summarized in Table 3.

Table 3
The model parameters determined by the present model

CWM	$F_0 \times 10^{18}$ (J)	α (−)
CWM-A1 [a]	0.183	1.034
CWM-A2 [b]	2.16	1.027
CWM-A3 [c]	11.3	1.020
CWM-A4	10.0	1.057
CWM-B1	6.01	1.104
CWM-B2	6.01	1.110
CWM-B3	6.01	1.115

[a] pH 8.1. [b] pH 9.4. [c] pH 10.1.

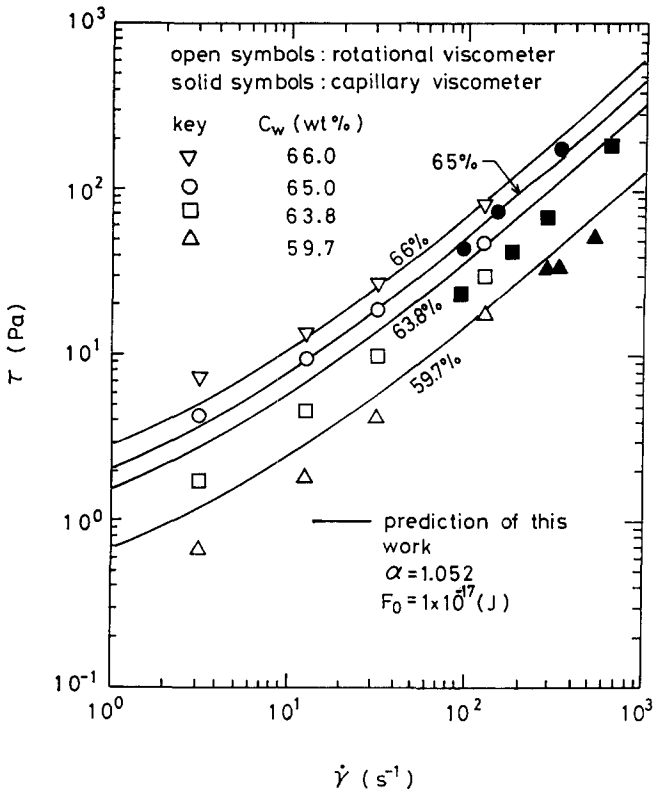

Fig. 9. Effect of coal concentration on CWM rheology.

Using these values of F_0 and α, shear stress vs. shear rate relationship was predicted for different concentration of CWM-A4. The predicted results indicated by solid lines in Fig. 9 show good agreement with experimental data. Thus we can conclude that once the model parameters are determined for one concentration condition, we can predict the flow characteristic of the same CWM at a different concentration. There may be a significant error if we apply this method to predict the rheology of a very different concentration. In such a case, the value of α may be changed if we go outside the range of prediction. Also, it must be noted that a single value of F_0 is enough to describe the concentration effect. This fact is reasonable because the change of solid concentration does not change the surface characteristics.

5.4. *Effect of surface condition on CWM viscosity*

The parameter F_0, i.e. inter-particle bonding energy, defined by the present model should depend on surface conditions. Here, the effect of pH on the rheology of CWMs is discussed. Usui and Sano reported the rheological data of CWM at different pH conditions in a previous paper [14]. Using the data of the same sample (CWM-A1, A2 and A3), rheology data were obtained as shown in Fig. 10.

Following the same procedure described in the previous section, the value σ of F_0 and the number α were determined for each pH condition. The values of the two parameters are summarized in Table 3. The predicted lines for each pH condition using Eq. (13) are shown in Fig. 10. Agreement between predictions and the experimental data implies that the present model can be successfully employed to estimate the effect of surface conditions on CWM rheology. However, it is noted that the values of α and F_0 must be determined for each surface condition. Also the value of F_0 must be tested in a future study whether this value is physically reasonable or not.

5.5. *Stress overshoot and stress undershoot caused by sudden change of shear rate*

Stress overshoot or stress undershoot has been observed for CWMs when the shear rate is suddenly changed [5]. Some examples using CWM-A2 are shown in Fig. 11. The solid circles correspond to the shear stress data obtained for constant shear condition. The open squares and open triangles correspond to stress overshoot and stress undershoot data, respectively, from the corresponding equilibrium stress level. The broken line was calculated following the present model. The number of minimum-sized particles in a cluster is assumed to remain unchanged during a sudden change of shear rate. If the value of n is constant, the slurry must show a Newtonian behaviour according to the present model. Thus the stress overshoot and stress undershoot data must fall in the Newtonian rheogram through

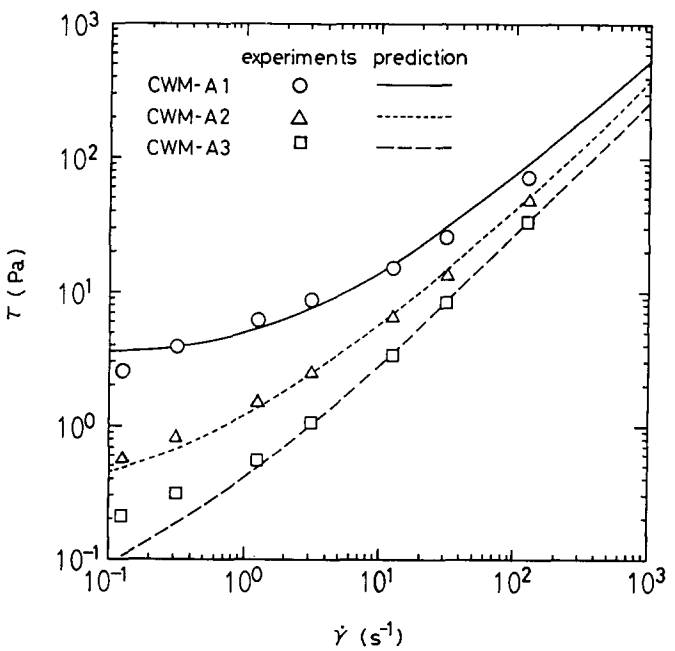

Fig. 10. Effect of surface condition on CWM rheology.

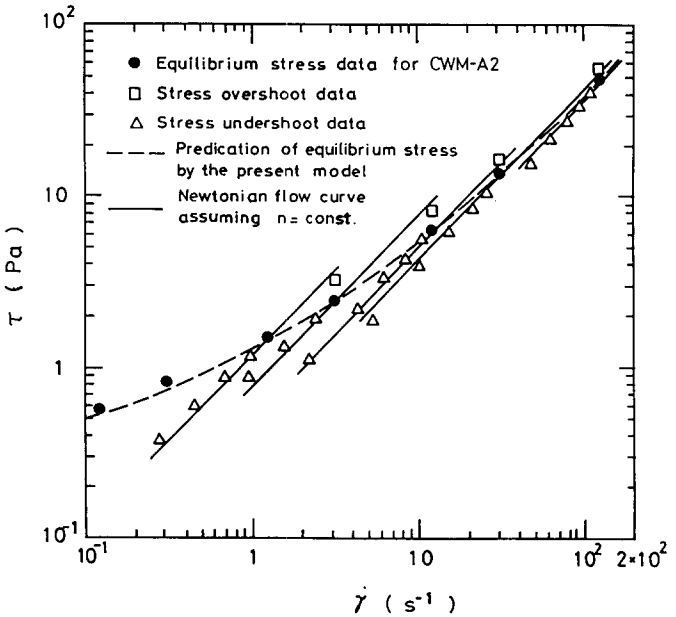

Fig. 11. Prediction of stress overshoot and stress undershoot by the present model.

the equilibrium stress level indicated by solid circles in Fig. 11. The solid lines in Fig. 11 were drawn following this idea, and agreement with the experimental results indirectly confirms the soundness of the present model.

5.6. *Thixotropic hysteresis observed during the linear increase and decrease of the shear rate*

A thixotropy model must predict the instantaneous stress level of a CWM if the shear history is specified. To examine this point, the following shear history was considered:

$\dot{\gamma}$ = sufficiently high to certify that $n = 1$ at $t < 0$

$\dot{\gamma} = 0$ at $0 < t < T_{\text{wait}}$

$\dot{\gamma} = 0.52t$ at $240s > t > T_{\text{wait}}$.

$\dot{\gamma} = 124.8 - 0.52t$ at $t > 240$ s.

The integration of Eq. (13) was done following the shear history mentioned above to give the change of shear stress. The calculated results for the CWM-A2 are compared with experimental results as shown in Fig. 12. As the waiting time is increased, the initial stress level in the experimental result is increased. According to the shear break-up of internal structure, the experimental data converge to a single flow curve. The predicted results of this work show the increase of stress level at a very low shear rate range in accordance with the increase of waiting time. However,

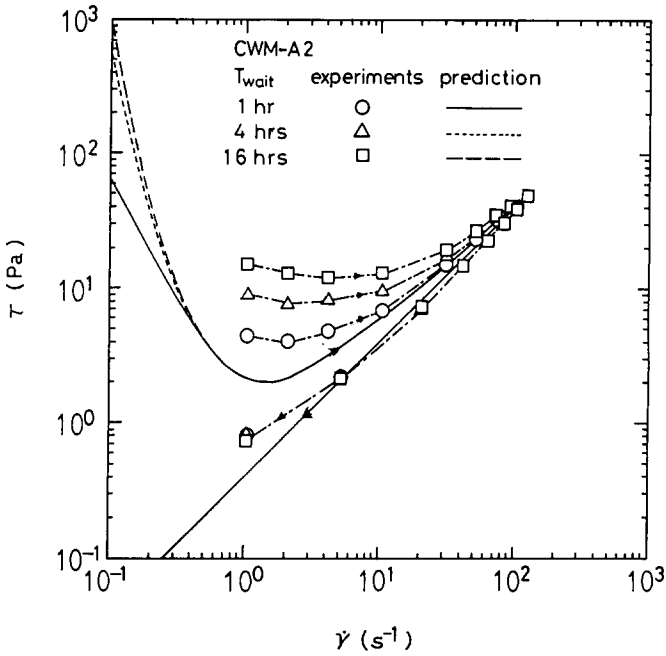

Fig. 12. Comparison of stress history predicted by the present thixotropy model and experimental results.

predicted curves converge to a single curve very rapidly. This means that the present thixotropy model over-estimates the shear break-up process. The shear break-up term in Eq. (13) is proportional to the second power of shear rate. Usui and Sano [5] suggested that the first power of shear rate appearing in the shear break-up term of a phenomenological thixotropy model was adequate for the prediction of thixotropic behavior of a CWM. More improvement in the shear break-up process must be carried out in the further study of CWM thixotropy.

It is evident that the flow characteristics of CWM seem to be nearly Newtonian when the shear rate is linearly decreased. The predicted line at the decreasing shear rate region was based on the assumption that the minimum size particles in a cluster remained constant, because the build-up process of internal structure needed a longer time. The prediction is in good agreement with experiments.

6. Concluding remarks

A thixotropy model was proposed for high-concentration slurries. The number of minimum-sized particles contained in a cluster was taken as a thixotropy parameter. The proposed model could be used to predict successfully the rheology of CWMs taking into account the effects of coal concentration, particle size distribution and surface conditions. However, a better knowledge of the break-up process of clusters is needed to verify the effectiveness of the model.

Acknowledgements

This work was supported by Grant-in-Aid for Scientific Research (No. 05044105 and No. 06650860) from the Ministry of Education, Science and Culture of Japan, for which the author expresses his sincere thanks. T. Saeki and Y. Toda deserve many thanks for their technical help in this work.

References

[1] Papers presented at 18th Int. Tech. Conf. on Coal Utilization and Fuel Systems, 26–29 April 1993, Clearwater, Florida, Pittsburgh Energy Tech. Center, Pittsburgh, PA, 1993.
[2] Papers presented at 9th Annual Int. Pittsburgh Coal Conf., 12–16 October 1992, University of Pittsburgh, PA, 1992.
[3] Papers presented at Japan-Australia-China Joint Symp. on Preparation and Transportation of Coal Slurries, 2–3 September 1993, Yamaguchi University, Japan, 1993.
[4] Papers presented at IEA-CLM Workshop on Coal Water Mixtures, 17–19 October 1994, NEDO, Japan, 1994.
[5] H. Usui and Y. Sano, Thixotropy of a coal water mixtures, J. Chem. Eng. Jap., 18 (1985) 519–525.
[6] D.C.-H. Cheng and F. Evans, Phenomenological characterization of the rheological behavior of inelastic reversible thixotropic and antithixotropic fluids, Brit. J. Appl. Phys., 16 (1965) 1599–1617.
[7] H. Usui, T. Saeki and Y. Sano, Stability evaluation of coal–water mixtures by internal structural stress, J. Chem. Eng. Jap., 21 (1988) 602–607.
[8] D.L. Swift and S.K. Friedlander, The coagulation of hydrosis by Brownian motion and laminar shear flow, J. Colloid Sci., 19 (1964) 621–647.
[9] K. Higashitani and G. Matsuno, Coagulation of colloidal particles in a simple shear flow (in Japanese), Proc. 14th Autumn Meeting of Soc. Chem. Eng. Jap., 2 (1980) 439–440.
[10] Lee, D.I., Packing of spheres and its effect on the viscosity of suspensions, J. Paint Technol., 42 (1970) 579–587.
[11] P.G. Smith and T.G.M. van De Ven, Shear-induced deformation and Rupture of suspended solid/liquid clusters, Colloids Surfaces, 15 (1985) 191–210.
[12] J. Happel, Viscosity of suspensions of uniform spheres, J. Appl. Phys., 28 (1957) 1288–1292.
[13] H. Usui, Y. Sano, M. Sawada and T. Hongoh, Adjustment of particle size distribution for the preparation of highly loaded coal-water slurries with reduced viscosity, J. Soc. Chem. Eng. Jpn., 12 (1986) 51–56.
[14] H. Usui and Y. Sano, Thixotropy of highly loaded coal–water mixtures, J. Soc. Rheol. Jpn. 14 (1986) 123–127.